

Document downloaded from:

<http://hdl.handle.net/10251/183614>

This paper must be cited as:

Fuentes López, C.; Ruiz Rico, M.; Fuentes López, A.; Barat Baviera, JM.; Ruiz, MJ. (2021). Comparative cytotoxic study of silica materials functionalised with essential oil components in HepG2 cells. *Food and Chemical Toxicology*. 147:1-12.
<https://doi.org/10.1016/j.fct.2020.111858>



The final publication is available at

<https://doi.org/10.1016/j.fct.2020.111858>

Copyright Elsevier

Additional Information

Comparative cytotoxic study of silica materials functionalised with essential oil components in HepG2 cells

Cristina Fuentes^{a1}, María Ruiz-Rico^a, Ana Fuentes^a, José Manuel Barat^a, María José Ruiz^b

^aDepartment of Food Technology, Universitat Politècnica de València. Camino de Vera s/n, 46022, València, Spain

^bLaboratory of Toxicology, Faculty of Pharmacy, Universitat de València, Av. Vicent Andrés Estellés s/n, 46100 Burjassot, València, Spain

¹**Corresponding author** Cristina Fuentes. Department of Food Technology, Universitat Politècnica de València. Camino de Vera s/n, 46022, Valencia, Spain: crifuel@upvnet.upv.es

Abbreviations

AB, Alamar Blue; APTES, (3-aminopropyl)triethoxysilane; ATP, Adenosine triphosphate; CTAB, Hexadecyltrimethylammonium bromide; DMEM, Dulbecco's modified eagle medium; DMSO, Dimethyl sulfoxide; DNA, Deoxyribonucleic acid; EDTA, Ethylenediaminetetraacetic acid; EFSA, European food safety authority; EOCs, Essential oil components; FADH, Flavin adenine dinucleotide semiquinone; FDA, US Food and drug administration; FMNH, Flavin mononucleotide semiquinone; GRAS, Generally recognized as safe; MCM-41, Mobile crystalline material-41; MTT, Thiazolyl blue tetrazolium bromide; NADH, Nicotinamide adenine dinucleotide reduced form; NADPH, Nicotinamide adenine dinucleotide phosphate reduced form; NBCS, Newborn calf serum; PBS, Phosphate buffered saline; ROS, Reactive oxygen species; SAS, Synthetic amorphous silica; SEM, Standard error of the mean; TEAH₃, Triethanolamine; TEM, Transmission electron microscopy; TEOS, Tetraethylorthosilicate; TGA, Thermogravimetric analysis.

Abstract

This work evaluated the cytotoxic effect of different EOCs-functionalised silica particle types. The *in vitro* toxicity of eugenol and vanillin-immobilised SAS, MCM-41 microparticles and MCM-41 nanoparticles was evaluated on HepG2 cells, and compared to free EOCs and pristine materials. The results revealed that free essential oil components and bare silica had a mild cytotoxic effect on HepG2 cells. However, the comparative study showed that free eugenol and vanillin had a milder cytotoxic effect than the equivalent concentrations of immobilised components on the different silica particles, while differences in cell viability between the bare and functionalised particles relied on the type of analysed material. The most cytotoxic materials were eugenol and vanillin-functionalised MCM-41 micro with IC_{50} values of 0.19 and 0.17 mg/mL, respectively, at 48 h exposure. Differences in cytotoxicity between functionalised particles may be attributed to the density of the functional components on their surface as a result of the functionalisation reaction performance for different materials. The study of the physico-chemical properties of particles demonstrated that cationic nature and increased hydrophobicity could be responsible for promoting cell-particle interactions for the eugenol and vanillin functionalised silica particles, enhancing their cytotoxic behaviour.

Keywords: MCM-41; silica; eugenol; vanillin; cytotoxicity; HepG2

1. Introduction

Synthetic amorphous silica (SAS), in its fumed and hydrated forms, is a food additive (E551) authorised to be directly used in dry-powered food formulations and tablets as anticaking and antifoaming agents, or as a carrier in the preparation of food additives and nutrients (EU Commission, 2011a). For decades, SAS has been used with no clear evidence for adverse health effects. In fact a recent re-evaluation of the safety of SAS by the EFSA Panel on Food Additives concluded that, based on available evidence, there was no indication of adverse effects for the reported uses and usage levels (Younes et al., 2018). However, the EFSA Panel emphasised the importance of considering the physico-chemical characteristics of the tested materials in their risk assessment as they may affect their biological behaviour. For this reason, any new SAS product that does not comply with specifications for bulk forms, or is designed for new technological functions in food, will require specific safety and risk assessments (Fruijtier-pöllöth, 2016). Several authors have demonstrated that different types of surface chemical modifications induce distinct toxicological responses *in vitro*. Santos et al. (2010) studied the cytotoxicity of SAS microparticles on Caco-2 cells and found that the two main factors to affect cell viability were particle size and surface chemistry treatment. Thermally oxidised, thermally carbonised and thermally hydrocarbonised mesoporous silicon microparticles induce different toxic responses, and these effects are attributed to cell-particle surface interactions, which cause mitochondrial disruption as a result of ATP depletion and reactive oxygen species (ROS) production. Other processes, such as cellular uptake and localisation, are also regulated by different surface modifications (Slowing et al., 2006). Puerari et al. (2019) have demonstrated that primary and tri-amine functionalised SAS nanoparticles are more cytotoxic than pristine material to Vero cells due to increased ROS production and lipid peroxidation. These

authors have hypothesised that functionalisation promotes a *Trojan horse effect*, by means of which cells recognise molecules on the material's surface as nutrients, which facilitates entry in the cytosol. Conversely to this study, Yoshida et al. (2012) have found that functionalisation of nanosilica with amine or carboxyl groups results in lower cytotoxicity, ROS production and DNA damage in different cell lines, suggesting the surface functionalisation of silica nanoparticles to be a useful tool for developing safer materials.

The development of antimicrobial agents based on the immobilisation of essential oil components (EOCs) on the surface of different silica particles has emerged as a new tool to improve EOCs' antimicrobial activity and to reduce their sensorial impact on foods. These materials have proven effective against different bacteria, moulds and yeast *in vitro* (Ruiz-Rico et al., 2017), as part of different food matrices (Ribes et al., 2017), or as filtering aids for beverages (Peña-Gómez et al., 2020). At this point, the potential application of these emerging materials in the food industry requires toxicological studies to identify any possible hazards for human health associated with their use. In this context, the present work aimed to compare the cytotoxic effect of three different types of functionalised silica particles, designed as antimicrobial systems, to be applied in the food industry. In particular, the *in vitro* toxicity of eugenol and vanillin-immobilised SAS microparticles, MCM-41 microparticles and MCM-41 nanoparticles was evaluated on HepG2 cells and compared to the effect of free EOCs and pristine materials.

2. Material and methods

2.1. Reagents

All the reagents and cell culture components were of standard laboratory grade. Synthetic amorphous silica (SAS) microparticles (SYLYSIA® SY350/FCP) were provided by Silysiamont (Italy). Acetonitrile, KOH, MgSO₄, HCl, CHCl₃, n-butanone, H₂SO₄ and dimethyl sulfoxide (DMSO) were obtained from Scharlab (Spain). Vanillin (MW: 152.2 g/mol, purity ≥ 99%) was supplied by Ventós (Spain). Thiazolyl blue tetrazolium bromide (MTT), glycine, eugenol (MW: 164.2 g/mol, purity ≥ 98%), (3-aminopropyl)triethoxysilane (APTES), triethanolamine (TEAH₃), tetraethylorthosilicate (TEOS), hexadecyltrimethylammonium bromide (CTAB), NaOH, and all other reagents used in the synthesis and functionalisation of silica particles, were purchased from Sigma-Aldrich (Spain). Alamar Blue® (AB) reagent was acquired from Invitrogen (USA). Trypsin-EDTA 0.5%, antibiotics, newborn calf serum (NBCS), phosphate buffered saline (PBS) and Dulbecco's Modified Eagle Medium (DMEM-Glutamax™) with high glucose (4.5 g/L) and sodium pyruvate were supplied by Gibco (LifeTechnologies, USA).

Stock solutions of eugenol and vanillin (2.5 M) were prepared in DMSO and were left frozen until used. The final tested eugenol and vanillin concentrations were achieved by adding them to the culture medium at a final DMSO concentration ≤ 0.5% (v/v).

2.2. Cell culture

Human hepatocarcinoma (HepG2) cells (ATCC: HB-8065) were cultured in DMEM-Glutamax medium supplemented with 10% NBCS, 100 U/mL penicillin and 100 µg/mL streptomycin. The incubation conditions were pH 7.4, 5% CO₂ at 37°C and 95% air

atmosphere at constant humidity. Cells were subcultured routinely twice weekly with only a few subpassages (< 40 subcultures) to maintain genetic homogeneity. HepG2 cells were subcultured after trypsinisation at the 1:3 split ratio. The medium was changed every 2-3 days. Absence of mycoplasma was checked routinely with the MycoAlert™ PLUS Mycoplasma kit (Lonza Rockland, USA).

2.3. Silica particles

2.3.1. Synthesis of MCM-41 particles

The synthesis of both types of MCM-41 mesoporous silica particles was performed using TEOS as the hydrolytic inorganic precursor and CTAB as the cationic surfactant agent. MCM-41 microparticles (MCM-41 micro) were synthesised by the “atran route” using a molar ratio solution of 7 TEAH₃: 2 TEOS: 0.52 CTAB: 0.5 NaOH: 180 H₂O. Briefly, TEAH₃ and NaOH were heated to 120 °C with stirring, the temperature was lowered to 70 °C and TEOS was slowly added. After heating the mixture to 118 °C, the temperature was lowered to 70 °C, water was added and the white suspension that formed was stirred for 1 h without heating before being aged at 100 °C for 24 h. For the synthesis of MCM-41 nanoparticles (MCM-41 nano), 1 g of CTAB was dissolved in 480 mL of deionised water with stirring. Then a solution of 7 mM of NaOH was added and the mixture was heated to 80 °C. Stirring was increased and 22.4 mM of TEOS solution was added dropwise. The reaction was left stirring for 30 min and neutralised with 4 mL of HCl 1 M. For both materials, particles were recovered by centrifugation, washed repeatedly with deionised water and ethanol, and oven-dried at 70 °C. Then dried solids were calcined at 550 °C for 5 h to remove the template.

2.3.2. Silica particles functionalised with EOCs

The functionalisation of SAS, MCM-41 micro and MCM-41 nano with eugenol and vanillin was carried out by the method developed by García-Ríos et al. (2018). This method consists in a three- and two-stage protocol for eugenol and vanillin, respectively, as the presence of an aldehyde group in the vanillin structure avoids the first stage. Firstly, eugenol was transformed into its aldehyde derivative by a Reimer-Tiemann reaction. For this purpose, 22 mM of eugenol were dissolved in 150 mL of water at 80 °C. The mixture was cooled at 60 °C, and 400 mM of KOH and 88 mM of CHCl₃ were slowly added, the latter at a rate of 1 mL/h. The solution was stirred at 60 °C overnight. Next it was cooled and acidified with 50 mL of 10% H₂SO₄. The purification of the eugenol aldehyde was carried out by extraction with n-butanone and rotary evaporation. In a second stage, the alkoxysilane derivatives of eugenol and vanillin were formed via the reaction of the eugenol aldehyde or pure vanillin dissolved in dichloromethane, with 20 mM of APTES for 1 h at 38 °C under reflux. Then solutions were rotary evaporated at 30 °C. In a third stage, the alkoxysilane derivatives were immobilised on the surface of the different silica particles. For this purpose, 5 g of SAS, 5 g of MCM-41 micro or 1.5 g of MCM-41 nano were added to 120 mL of acetonitrile and the reaction was stirred for 5.5 h at room temperature. After centrifugation, the reduction of the imine bond of the vanillin functionalised materials was performed by adding an excess of sodium borohydride in 150 mL of methanol and stirring overnight. Finally, particles were washed with acetonitrile and distilled water (eugenol-functionalised materials), or with pH 4 distilled water (vanillin-functionalised materials), and dried in a vacuum for 12 h at room temperature.

2.3.3. Physico-chemical characterisation of silica particles

The bare and EOCs-functionalised silica materials were characterised by standard instrumental techniques. The morphological analysis of the silica materials was performed by transmission electron microscopy (TEM) with a Philips CM 10 microscope (Koninklijke Philips Electronics N.V, The Netherlands) operating at 80 kV. A Zetasizer Nano ZS (Malvern Instruments, UK) was used to determine the zeta potential of particles. This parameter was calculated from the particle mobility values using the Smoluchowski model. Particle size distribution was determined by a Malvern Mastersizer 2000 (Malvern Instruments, UK) and by applying the Mie theory (refractive index of 1.45, absorption index of 0.01 for SAS and 0.1 for the MCM-41 materials). For the zeta potential and particle size distribution measurements, samples were dispersed in distilled water and sonicated for 2 min.

Thermogravimetric analysis (TGA) and elemental analyses were performed to quantify the concentration of the EOCs immobilised on the surface of the functionalised particles. The TGA was carried out on a TGA/SDTA 851e Mettler Toledo scale (Mettler Toledo Inc., Switzerland) in an oxidising atmosphere (air, 80 mL/min) with a heating programme (heating ramp of 10 °C/min from 25 °C to 1,000 °C) and a heating stage. The elemental analysis for C, H and N was carried out by a combustion analysis in a CHNOS Vario EL III model (Elemental Analyses System GMHB, Germany).

2.4. *In vitro* cytotoxicity

Cytotoxic effects were determined in HepG2 cells by the MTT and AB assays. They have been extensively used in *in vitro* toxicological studies to measure cell proliferation and survival. In the MTT assay, the soluble yellow tetrazolium salt is reduced to insoluble purple formazan by the mitochondrial NADH dehydrogenases present in

viable cells (Holst & Oredsson, 2005) . The AB assay determines cells' viability by reducing non-fluorescent blue resazurin, but only in the metabolically active cells, to a fluorescent pink resorufin. Due to the oxidation-reduction potential of resazurin, it can be reduced by all the components of the cellular respiration metabolic reactions (NADPH, FADH, FMNH, NADH as well as cytochromes), but also by the other enzymes located in the cytoplasm and mitochondria, such as reductases and diaphorases (Rampersad, 2012). Both redox assays determine cell viability by quantifying the metabolic activity of cells. However, while AB reduction is the result of multiple metabolic reactions within the cell, the MTT assay indicates a mitochondrial dysfunction (Davoren et al., 2007).

The MTT assay was performed according to Ruiz et al. (2006). Briefly, the HepG2 cells were grown in 96-well culture plates at a density of 1×10^5 and 3×10^4 cells/mL for 24-hour and 48-hour experiments, respectively. After cells reached 80% confluence, the culture medium was replaced with fresh medium containing serial dilutions of the tested compounds: from 0.3 to 5 mM (eugenol), from 0.9 to 15 mM (vanillin), from 0.11 to 28.5 mg/mL (bare SAS) and from 0.14 to 18.3 mg/mL (bare MCM-41 micro and MCM-41 nano). After 24 h or 48 h of exposure, the medium was removed and 200 μ L of fresh medium were added to each well. Then 50 μ L of MTT were added per well, and plates were returned to the incubator in the dark at 37 °C, 5% CO₂ for 3 h. Next the MTT solution was discarded and 200 μ L of DMSO were added, followed by 25 μ L of Sorensen's glycine buffer (glycine 0.1M, NaCl 0.1M, pH: 10.5 with 0.1 M NaOH). Plates were gently shaken for 10 min to achieve complete dissolution. Absorbance was measured at 570 nm by an automatic ELISA plate reader (Victor 3TM 1420, PerkinElmer, USA).

The cytotoxic effect of the functionalised materials was simultaneously determined by the AB and the MTT assays. When both methods were used, they were performed consecutively in the same plate, as described by Efeoglu et al. (2017). After growing cells on 96-well culture plates for 24 h, wells were washed with 100 μ L of PBS and 100 μ L of the test solution were added. Different ranges of the concentrations of the eugenol and vanillin functionalised SAS (0.02-10 mg/mL), eugenol functionalised MCM-41 micro and nano (0.005-2.5 mg/mL) and vanillin functionalised MCM-41 micro and nano (0.004-2 mg/mL) were assayed. Plates were incubated for 24 h or 48 h. During this time, neither the medium was, nor the tested compounds were, replenished. After incubation, the medium was removed and wells were washed with 100 μ L of PBS. Then 100 μ L of non-supplemented DMEM medium with 10% MTT stock solution (5 mg/mL in PBS) and 5% AB solution (v/v) were added. Plates were incubated (37°C, 5% CO₂, 3 h) and AB fluorescence was measured ($\lambda_{\text{excitation}}=540$, $\lambda_{\text{emission}}=595$ nm) by a microplate reader fluorometer (Fluoroskan Ascent, Fisher Scientific, Spain). Subsequently for the MTT assay, wells were washed with PBS and 100 μ L of DMSO were added. Then plates were shaken at 240 rpm for 10 min and absorbance was quantified at 570 nm.

For all the experiments, the control samples of each particle type were prepared by incubating the medium with particles in a non-cellular environment at all the tested concentrations (cell-free controls). All the solutions were prepared immediately prior to use and particles' suspensions were sonicated for 5 min before the experiments.

The final absorbance of the treated and unexposed cell wells was corrected for particle interference by subtracting the absorbance of the cell-free controls from the absorbance of the test wells.

For both the MTT and AB assays, cell viability was expressed as a percentage in relation to the control solvent (0.5% DMSO). Data were presented as the mean (SEM)

of three independent experiments. The mean inhibition concentration (IC_{50}) values were calculated whenever possible by a non-linear regression test using version 8.0.1 of the GraphPad Prism software (GraphPad Software, USA).

2.5. Comparative evaluation of the toxic effects of EOCs, bare and functionalised silica particles

The MTT assay was used to determine and compare the toxic effects of eugenol, vanillin and the bare and EOCs-functionalised SAS, MCM-41 micro and MCM-41 nano. In the comparative studies, concentration ranges were selected by considering the IC_{50} values of eugenol and vanillin previously determined. The equivalent concentrations of particles were established based on the EOCs content in the functionalised materials determined by the TGA and elemental analyses. The grams of EOCs per gram of particle were calculated according to Ruiz-Rico et al. (2017). The assayed concentrations of the different components are shown in Table 1.

Table 1. Concentrations assayed in the comparative study of the eugenol (Eu), vanillin (Va), and bare and functionalised SAS, MCM-41 micro and MCM-41 nano.

	Concentrations			
	A	B	C	D
Eugenol (mM)	0.5	1	2	4
Bare SAS (mg/mL)	14.07	28.16	56.3	112.6
Bare MCM-41 micro (mg/mL)	1.86	3.73	7.45	14.94
Bare MCM-41 nano (mg/mL)	1.45	2.90	5.18	11.62
Eu SAS (mg/mL)	14.16	28.3	56.6	113.3
Eu MCM-41 micro (mg/mL)	1.95	3.90	7.80	15.60
Eu MCM-41 nano (mg/mL)	1.53	3.07	6.14	12.28
Vanillin (mM)	1.25	2.5	5	10
Bare SAS (mg/mL)	6.65	13.3	26.6	53.18
Bare MCM-41 micro (mg/mL)	1.52	3.04	6.08	12.16
Bare MCM-41 nano (mg/mL)	1.88	3.76	7.54	15.07
Va SAS (mg/mL)	6.84	13.7	27.4	54.70
Va MCM-41 micro (mg/mL)	1.71	3.42	6.84	13.68
Va MCM-41 nano (mg/mL)	2.09	4.14	8.29	16.57

2.6. Statistical analysis

The statistical data analysis was carried out using Statgraphics Centurion XVI (Statpoint Technologies, Inc., Warrenton, VA, USA). The differences observed between the cells exposed to test solutions and the control were analysed by the

Student's *t*-test for paired samples. The differences between functionalised silica particles' components were analysed by a one-way analysis of variance (ANOVA), followed by the LSD (least significant difference) *post hoc* test for multiple comparisons. Statistical significance was considered at $p \leq 0.05$.

3. Results

3.1. Physico-chemical characterisation of silica particles

Figure 1 shows the morphological characterisation of the bare and EOCs-functionalised silica materials. An irregular globular shape for SAS, but irregular and elongated for the MCM-41 micro, and homogeneous and round-shape for the MCM-41 nano, was evidenced. The individual particle size measured by TEM was 2.24 (0.80) μm , 1.22 (0.93) μm and 73.70 (12.80) nm for the bare SAS, MCM-41 micro and MCM-41 nano, respectively. No differences in either morphology or size were observed between the bare and functionalised silica particles. Additionally, the TEM images showed the well-defined hexagonal pore structure of the mesoporous MCM-41 materials in the form of parallel lines, which created channels in the bare and modified particles and confirmed that the mesoporous structure was preserved after functionalisation.

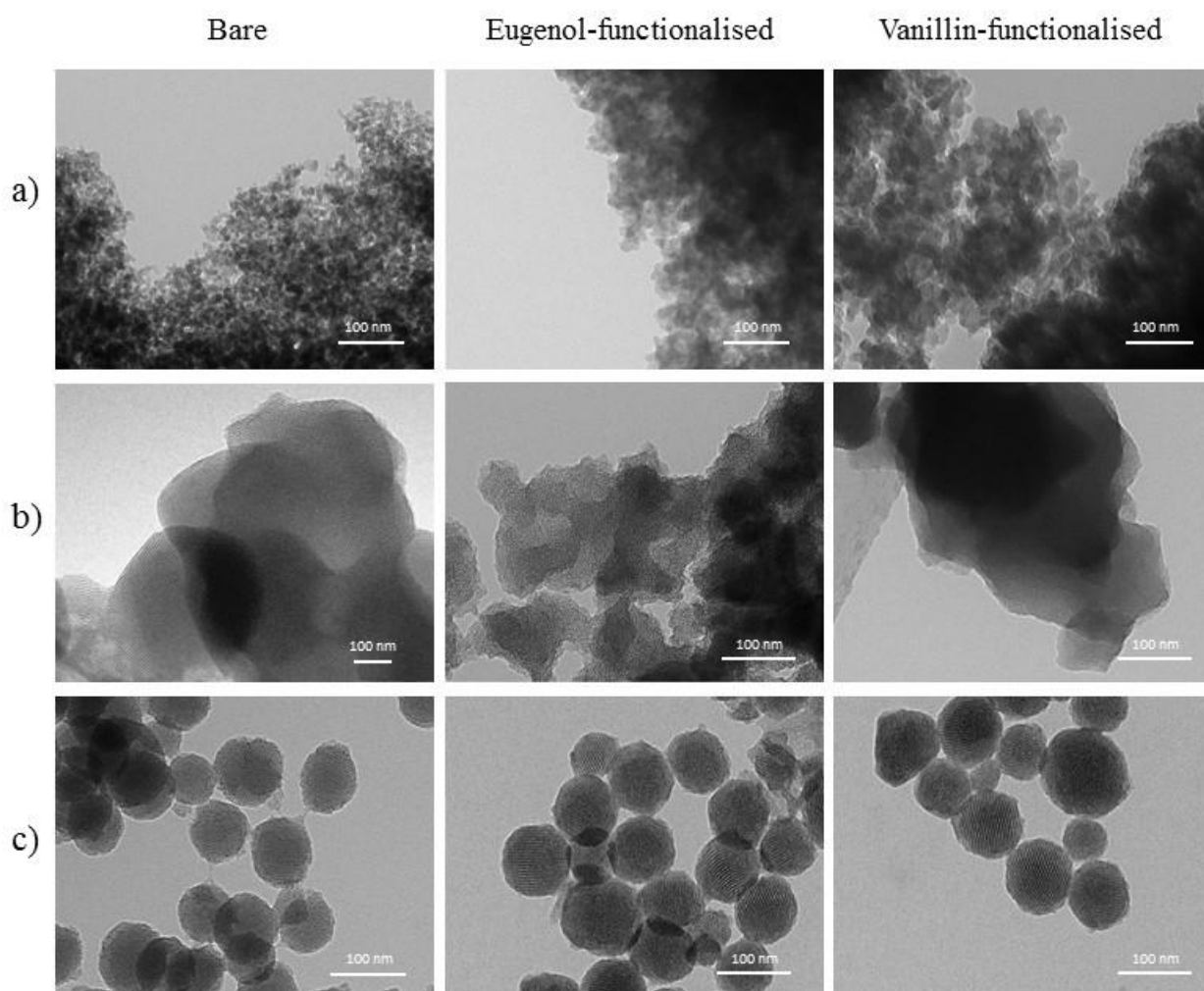


Figure 1. TEM images of the bare and EOCs-functionalised silica particles: a) SAS, b) MCM-41 micro and c) MCM-41 nano.

All the bare particles had negative zeta potential values due to the presence of silanol groups, while the functionalised materials presented positive values given the eugenol and vanillin alkoxy silane derivatives anchored to their surface (Table 2). This change in the zeta potential values confirmed the efficiency of the functionalisation method. Moreover, as all the particles analysed in this study were within or close to the instability range (+30 to -30 mV), formation of agglomerates and sedimentation of particles were expected.

The analysis of particle size distribution ($d_{0.5}$) showed that all the materials used in this study fell within the microscale size range (Table 2). The bare particles with the largest hydrodynamic particle size were the MCM-41 nano, followed by SAS and the MCM-41 micro. As the TEM analysis of the MCM-41 nano found a primary particle size within the range from 60 to 87 nm, these results denote the marked tendency of this type of material to form large agglomerates.

Table 2. Zeta potential (ZP) values and particle size distribution ($d_{0.5}$) of the different bare and EOCs-functionalised particles. Values are expressed as mean (SD) (n=3).

Particle type	Functionalisation	ZP (mV)	$d_{0.5}$ (μm)
SAS	Bare	-19.36 (2.15)	3.02 (0.05)
	Eugenol	9.39 (0.40)	3.13 (0.00)
	Vanillin	28.96 (1.15)	2.33 (0.00)
MCM-41 micro	Bare	-42.07 (0.56)	0.67 (0.00)
	Eugenol	8.07 (2.21)	0.64 (0.00)
	Vanillin	43.22 (3.45)	0.61 (0.00)
MCM-41 nano	Bare	-43.10 (0.25)	4.79 (0.00)
	Eugenol	19.10 (0.32)	2.99 (0.01)
	Vanillin	23.00 (0.35)	0.70 (0.00)

The amount of functionalised particles needed to obtain the equivalent concentrations of free EOCs during the cell viability assays was determined by the TGA and the elemental analysis. As shown in Table 3, SAS presented the least functionalisation performance from the three studied types of silica particles. In

addition, vanillin anchoring achieved higher functionalisation yields than eugenol, with differences of up to 5-fold bigger for SAS.

Table 3. Eugenol or vanillin content (α) in the functionalised SAS, MCM-41 micro and MCM-41 nano.

Particle type	α_{eugenol} (g/g SiO₂)	α_{vanillin} (g/g SiO₂)
SAS	0.0062	0.0318
MCM-41 micro	0.0479	0.1550
MCM-41 nano	0.0642	0.1130

3.2. Cell viability assays

3.2.1. IC₅₀ determination of EOCs, bare and functionalised materials

The cytotoxic effect of the eugenol, vanillin and bare silica particles on HepG2 cells was evaluated by the MTT assay for 24 h and 48 h to determine the molar concentration that reached 50% inhibition of cellular proliferation (IC₅₀). The concentration-response curves for the different components after 24 h and 48 h of exposure are shown in Figures 2 and 3.

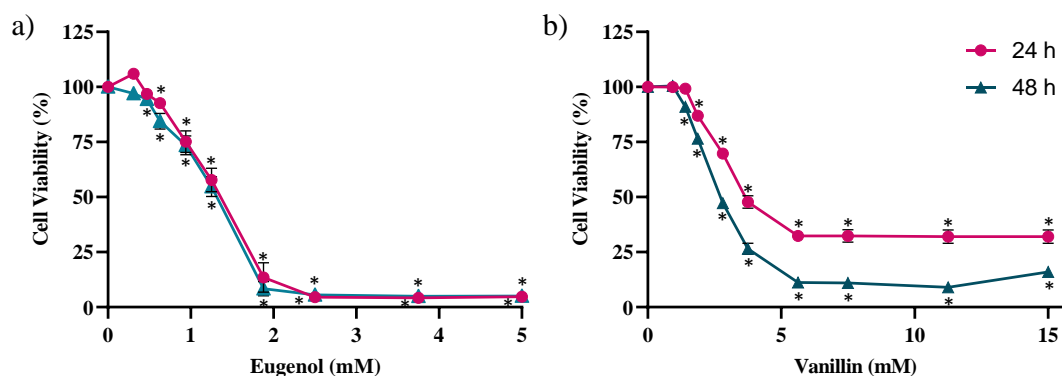


Figure 2. Concentration-effect curves of eugenol (a) and vanillin (b) in HepG2 cells after 24 h and 48 h of exposure by the MTT assay. The results are expressed as a percentage of cell viability in relation to the untreated controls and are represented as the mean (SEM) of three independent experiments, each carried out 6-fold. (*) $p \leq 0.05$ indicates significant differences compared to the control.

Cells exposed to eugenol and vanillin revealed diminished cell viability in a concentration-dependent manner (Fig. 2), with eugenol being the most cytotoxic essential oil in HepG2 cells. The IC_{50} values for eugenol were 1.29 (0.10) mM and 1.27 (0.10) mM at 24 and 48 h, respectively, while the IC_{50} values obtained by vanillin for both exposure times were 2.87 (0.13) mM and 2.53 (0.10) mM.

The cells exposed to bare silica particles presented reduced cell viability in a concentration-dependent manner by the MTT assay (Fig. 3). The bare SAS were the most cytotoxic in HepG2 cells, followed by the bare MCM-41 micro, and finally by the bare MCM-41 nano. The IC_{50} values for the bare SAS were 11.03 (3.52) mg/mL and 6.91 (1.78) mg/mL at 24 h and 48 h, respectively. Exposing HepG2 cells to the bare MCM-41 micro for 24 h and 48 h gave IC_{50} values of 18.90 (2.89) mg/mL and 15.82 (0.90) mg/mL, respectively. No IC_{50} value was obtained for the bare MCM-41 nano at

any tested time within the range of evaluated concentrations. Moreover, the concentration-effect curves of the bare silica particles showed that low SAS and MCM-41 micro concentrations brought about a stimulatory response of the mitochondrial function in HepG2 cells (Fig. 3a and 3b).

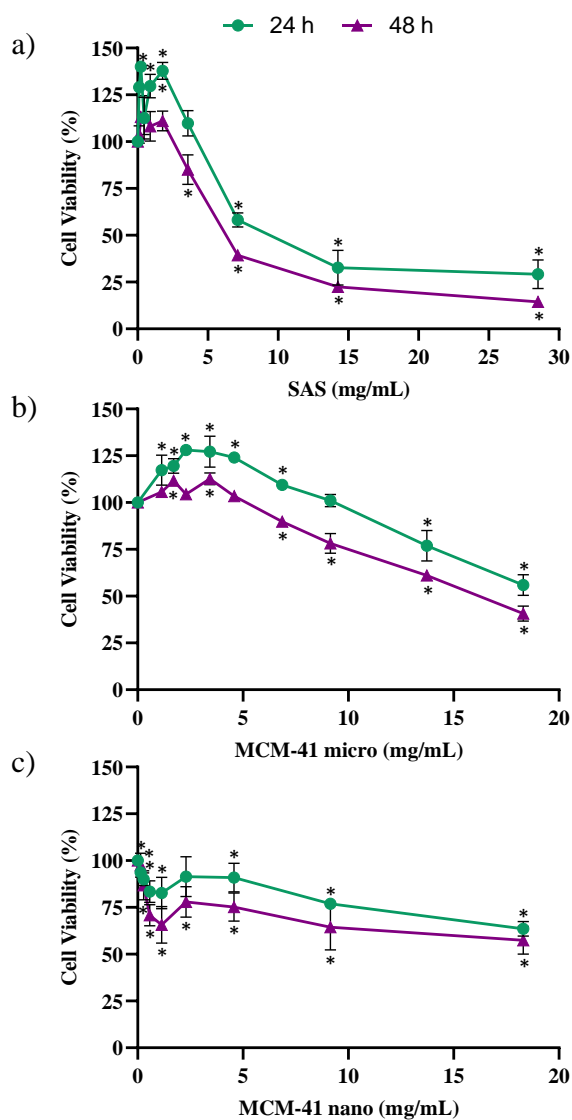


Figure 3. Concentration-effect curves of the bare SAS (a), bare MCM-41 micro (b) and bare MCM-41 nano (c) in HepG2 cells after 24 and 48 h of exposure by the MTT assay. The results are expressed as a percentage of cell viability in relation to the untreated controls, and are represented as the mean (SEM) of three independent experiments, each carried out 6-fold. (*) $p \leq 0.05$ indicates significant differences compared to the control.

The comparative effect related to cell viability between functionalised silica particles was evaluated in HepG2 cells by the MTT and AB assays at 24 h and 48 h of exposure. The concentration-response curves are shown in Figure 4.

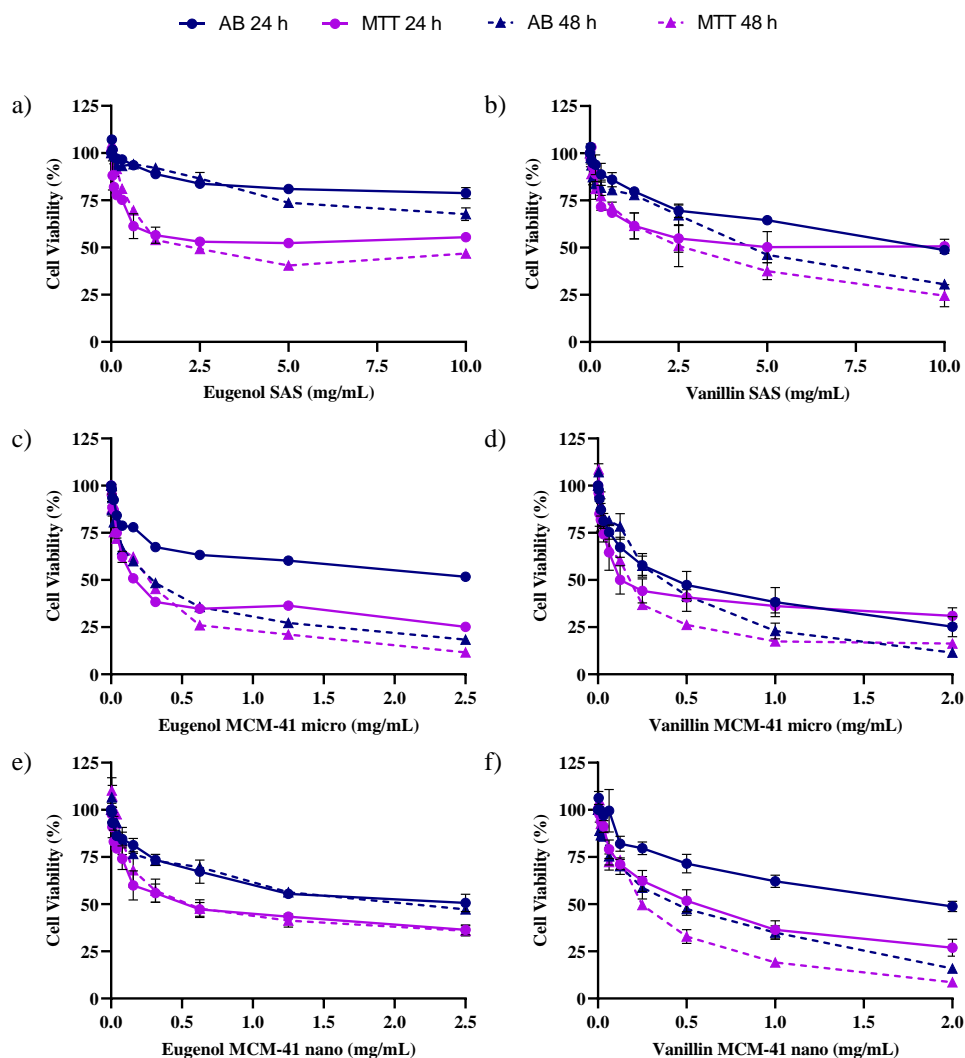


Figure 4. Concentration-effect curves of eugenol and vanillin functionalised SAS (a and b), MCM-41 micro (c and d) and MCM-41 nano (e and f) in HepG2 cells after 24 h and 48 h of exposure by the MTT and AB assays. The results are expressed as a percentage of cell viability in relation to the untreated controls, represented as the mean (SEM) of three independent experiments, each carried out 6-fold. (*) $p \leq 0.05$ indicates significant differences compared to the control.

The IC₅₀ values for the functionalised silica particles are shown in Table 4. The functionalised SAS particles displayed the least cytotoxic effect from the three types of silica materials, while functionalised MCM-41 micro were the most cytotoxic against HepG2 cells. In the case of MCM-41 nano the strongest cytotoxic effect was for the vanillin-functionalised particles after 48 h exposure. For the different functionalised materials, the strongest cytotoxic effect was observed by the MTT than by the AB assay according to the obtained IC₅₀ values.

Table 4. IC₅₀ (SEM, n=3) values of the eugenol and vanillin-functionalised silica in HepG2 cells by the MTT and AB assays at 24 h and 48 h of exposure.

EOCs-functionalised silica	Assay	IC ₅₀ (mg/mL)	
		Exposure time (h)	
		24	48
Eugenol SAS	MTT	5.45 (3.70)	3.18 (1.01)
	AB	> 10	> 10
Eugenol MCM-41 micro	MTT	0.24 (0.05)	0.19 (0.03)
	AB	2.47 (0.69)	0.27 (0.03)
Eugenol MCM-41 nano	MTT	0.58 (0.19)	0.68 (0.27)
	AB	2.32 (0.79)	1.93 (0.56)
Vanillin SAS	MTT	5.00 (3.00)	2.29 (0.69)
	AB	10.18 (2.91)	4.57 (1.36)
Vanillin MCM-41 micro	MTT	0.23 (0.09)	0.17 (0.03)
	AB	0.41 (0.10)	0.33 (0.06)
Vanillin MCM-41 nano	MTT	0.50 (0.10)	0.25 (0.03)
	AB	1.79 (0.74)	0.37 (0.07)

3.2.2. Comparative evaluation of the toxic effects of the EOCs, bare and functionalised silica particles

The concentration-response plots for the equivalent concentrations of the eugenol, eugenol-functionalised silica particles and bare silica particles in HepG2 cells after 24 h and 48 h of exposure are shown in Figure 5 (assayed concentrations are offered in detail in Table 1). Free eugenol exhibited a milder cytotoxic effect than eugenol-immobilised on silica particles' surface at concentrations below the IC_{50} value (concentrations A and B). When considering both exposure times, differences in cell viability between free eugenol and eugenol-functionalised materials ranged from 47% to 26% for SAS, and from 55% to 17% for the MCM-41 micro. Significant differences were also observed after 24 h of exposure to the lowest concentration of the eugenol functionalised MCM-41 nano (A). At the highest tested concentration (D), less than 94% of HepG2 cells survived after treatment with free eugenol or eugenol immobilised on SAS and MCM-41 nano at both exposure times.

Differences in cell viability between the bare and eugenol-functionalised particles depended on the analysed type of material. These differences ranged from 50% to 80% for the MCM-41 micro and from 43% to 57% for concentrations exceeding 6.14 mg/mL of the MCM-41 nano (C), whereas no significant differences in cell viability were observed for the lowest concentration (D) of the MCM-41 nano or SAS particles at any tested time. The eugenol-functionalised MCM-41 micro was significantly more cytotoxic than the bare MCM-41 micro at all the tested concentrations.

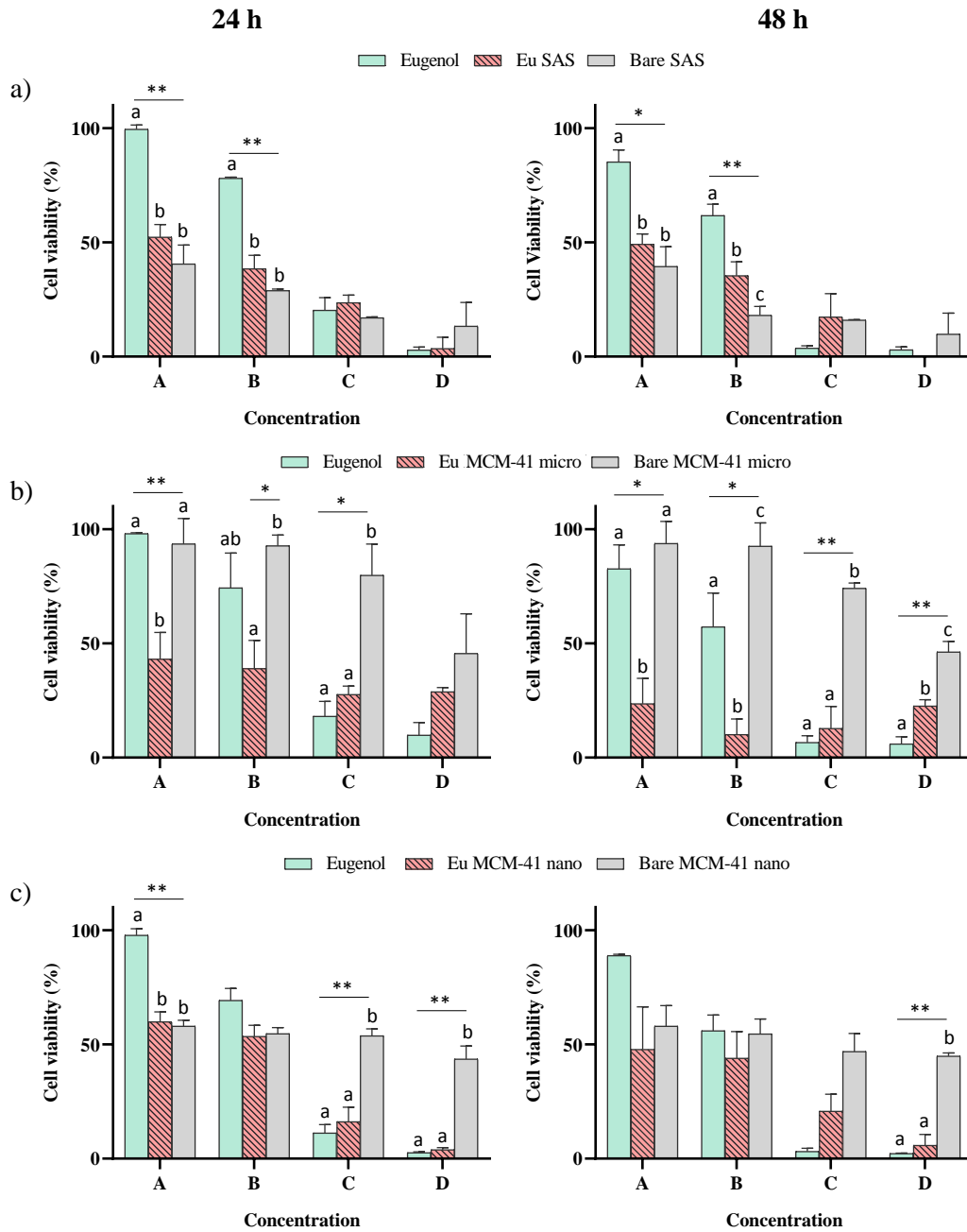


Figure 5. Concentration-cell viability plots of eugenol, bare and eugenol-functionalised SAS (a), MCM-41 micro (b) and MCM-41 nano (c) in HepG2 cells after 24 h and 48h of exposure by the MTT assay. The results are expressed as a percentage of cell viability in relation to the untreated controls, represented as the mean (SEM) of three independent experiments, each carried out 6-fold. The bars with different letters (a-c) indicate significant differences (** $p \leq 0.01$, * $p \leq 0.05$). The bars with no letters correspond to non-significant differences ($p > 0.05$).

The comparative study of the vanillin-functionalised particles and their components gave similar results to those obtained for eugenol (Fig. 6). Free vanillin was less cytotoxic than the equivalent vanillin concentrations anchored to the different silica particles at the two highest studied concentrations (concentrations A and B in Table 1). Differences between free vanillin and vanillin-functionalised materials ranged from 40% to 37% for SAS, from 78% to 4% for MCM-41 micro and from 76% to 3 % for MCM-41 nano after 24 h of exposure.

Both the bare and vanillin-functionalised silica particles presented a concentration-dependent effect on cell viability, but differences appeared depending on the type of material. No significant differences in cell viability were observed between the bare and vanillin functionalised SAS, but the vanillin-functionalised MCM-41 particles were significantly more cytotoxic than the bare MCM-41 at all the tested concentrations. The cell viability percentages ranged from 17% to 26% for 24 h exposure for the vanillin functionalised MCM-41 micro, while the bare MCM-41 micro only reduced cell viability to 57% at the maximum tested concentration. After exposure to the vanillin functionalised MCM-41 nano for 24 h and 48 h, cell viability ranged from 11% to 25% and from 8% to 22%, respectively. In contrast, bare MCM-41 nano did not present a concentration-dependent cytotoxic effect, and displayed a cell viability range from 45% to 59% after 24 h of exposure, and from 40% to 56% after 48 h.

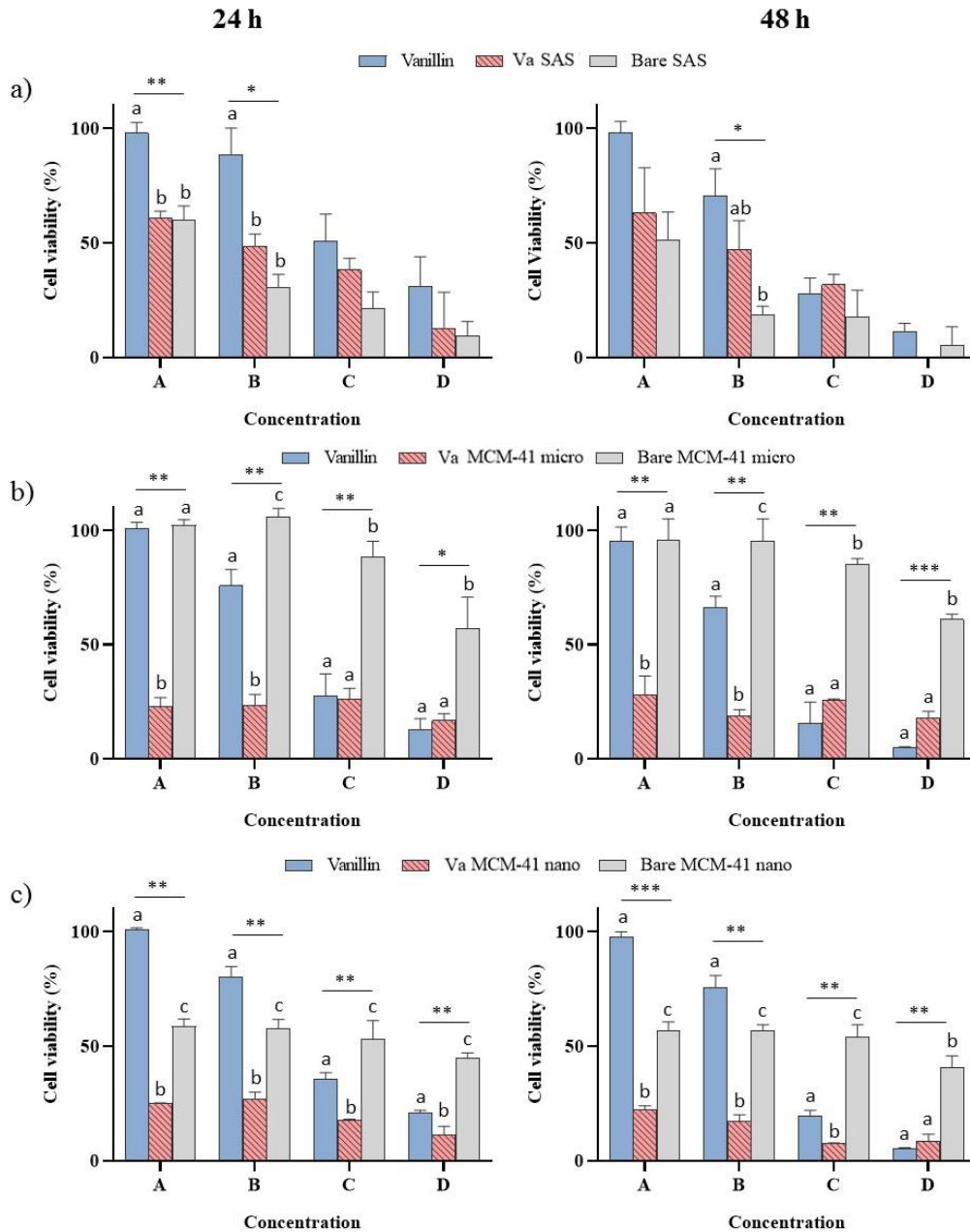


Figure 6. Concentration-cell viability plots of the vanillin functionalised SAS (a), MCM-41 micro (b) and MCM-41 nano (c) in HepG2 cells after 24 h and 48h of exposure by the MTT assay. The results are expressed as a percentage of cell viability in relation to the untreated controls, represented as the mean (SEM) of three independent experiments, each carried out 6-fold. The bars with different letters (a-c) indicate significant differences (** $p \leq 0.01$, *** $p \leq 0.001$), while the bars with no letters correspond to non-significant differences ($p > 0.05$).

4. Discussion

The presence of silanol groups on the surface of silica particles enables a wide variety of surface modifications by the covalent attachment of specific functional groups and organic molecules (Diab et al., 2017). This fact, along with their biocompatibility and low toxicity, make silica particles very interesting for designing hybrid materials in a number of oral applications (Bagheri et al., 2018; Ros-Lis et al., 2018). As surface properties are key factors for determining toxicological responses to particles (Vicentini et al., 2017), the study of the cytotoxicity aspects of modified silica structures will be crucial for successful applications.

Previously, the functionalisation of silica particles with EOCs has been demonstrated to prevent the degradation of materials under physiological conditions (Fuentes et al., 2020). However, lack of information about the toxicological behaviour of these materials indicates the need for specific toxicological evaluations. This paper describes the *in vitro* cytotoxicity assessment of different types of eugenol and vanillin-functionalised silica particles designed as antimicrobial systems to be applied in the food industry. This effect was compared with the cytotoxic behaviour of free EOCs and bare silica particles using HepG2 cells as an *in vitro* model system.

Eugenol and vanillin are both listed as “Generally Recognized as Safe” (GRAS) by the US Food and Drug Administration (FDA, 2020) and are included on the EU list of flavouring substances approved for use in foods without any specific restriction (EU Commission, 2011a). In this study, both EOCs reduced cell viability in a concentration-dependent manner. The cytotoxic effect on HepG2 cells was stronger with eugenol as vanillin presented an IC_{50} value, which increased by roughly 2-fold. A wide range of eugenol IC_{50} values can be found in the literature depending on the employed cell type. The IC_{50} values for eugenol ranged from approximately 0.75 mM in osteoblastic cells

(U2OS) (Ho et al., 2006) to 400 µg/mL (2.4 mM) in mesenchymal stem cells (MSCs) (Sisakhtnezhad et al., 2018) after 24 h of exposure, while an IC₅₀ value as high as 285 mM has been found for human submandibular gland carcinoma (HSG) after 48 h of exposure (Fujisawa et al., 2002). With vanillin, the IC₅₀ values after 72 h of exposure ranged from 200 µg/mL (1.31 mM) in HepG2 cells (Al-Naqeb et al., 2010) to 574.33 µg/mL (3.77 mM) in colorectal human cancer cells (HT-29) (Shakeel et al., 2016).

Bare silica materials also had a mild effect on HepG2 cell viability, as measured by the MTT assay. Some studies have suggested that the MTT method could fail to accurately predict the toxicity of mesoporous silica due to spontaneous redox reactions between particles and MTT (Braun et al., 2018). So cell-free controls were included in each experiment to avoid the potential influence of materials on cytotoxicity assays. The results evidenced no reaction between the MTT reagent and the bare MCM-41 particles, which could be explained by the completely oxidised SiO₂ surface of particles (Laaksonen et al., 2007).

Of the three different studied pristine particles, SAS was the most cytotoxic material, followed by MCM-41 micro and MCM-41 nano in that order. A mild cytotoxic effect was expected for the commercial SAS herein used as this hydrated silica form has been declared to meet the requirements for use in plastic, inks and other articles that are intended to come into contact with food according to EU regulations (EU Commission, 2011b). Despite the low SAS toxicity observed, our results were higher than those reported by Sakai-Kato et al. (2014), who studied the cytotoxicity of different sized SAS in Caco-2 cells by the WST-8 assay. These authors did not observe any cytotoxic effect for particles larger than 100 nm, not even at the 10 mg/mL concentration. In contrast, Reus et al. (2020) evaluated cytotoxic effects at high concentrations (0.192-7.750 mg/mL) of 100 nm of silica nanoparticles on a skin fibroblast cell line (BALB/c

3T3) by the neutral red uptake assay, which gave an IC₅₀ value of 1.99(0.24) mg/mL after 48 h of exposure. However, the results obtained in both studies are not completely comparable because of the physico-chemical differences in silica particles that may consequently affect their behaviour (Younes et al., 2018).

One of the most versatile classes of amorphous silica particles is mesostructured silica materials, such as MCM-41. Due to their biocompatibility, ordered pore structure, large surface area and high-density surface silanol groups, these materials show a high ability to be chemically modified, and are particularly useful tools for designing hybrid materials (Jaganathan & Godin, 2012). Several studies have evaluated cell viability after exposure to low concentrations of MCM-41 materials on different cell lines, and observed no cytotoxic effects (Giménez et al., 2015; Pérez-Esteve et al., 2016). However, very few studies have investigated the effect of high concentrations on cell viability. This is the case of Heikkilä et al. (2010), who studied the cytotoxicity of MCM-41 microparticles on Caco-2 cells as a model for oral drug delivery to be administered at frequent intervals. The MCM-41 particles induced cell membrane integrity damage, diminished cell metabolism and increased apoptotic signalling after a 24-hour treatment at concentrations of 1 mg/mL. The cytotoxic mechanisms of MCM-41 included an increase in ROS, especially superoxide radical ($O_2^{\cdot-}$) formation, a drop in cell antioxidant defences, and increases in both mitochondrial dysfunction and apoptotic signalling.

MCM-41 nano had the least effect on cell viability of the three bare silica particles studied. Literature data report higher cytotoxicity associated with silica nanomaterials compared to their micro-sized counterparts for non-phagocytic cells (Li et al., 2011). However, this effect has been described only for particles with a diameter below 100 nm (Sakai-Kato et al., 2014). The high surface area to volume ratio provides silica

nanoparticles with high surface energy, which is minimised by the formation of aggregates and agglomerates (Bantz et al., 2014; Seipenbusch et al., 2010). As previously mentioned, the bare MCM-41 nano presented an individual particle size range from 60 to 87 nm, but the largest hydrodynamic size of the three silica particles. Therefore, the lesser cytotoxic effect evidenced in MCM-41 nano could be related to their trend to form large agglomerates, which has been explained by reduced absorption by cells (Li et al., 2011).

Interestingly, the bare SAS and bare MCM-41 micro had an hormetic effect at the low tested concentrations. The biphasic concentration-response or hormetic effect, characterised by low concentration stimulation and a high concentration toxic effect, has been attributed to defensive and adaptive responses of cells to stress (Calabrese, 2008), and this effect has been previously reported for silica nanoparticles (Mytych et al., 2016; Reus et al., 2020).

The comparative analysis of EOCs, bare silica and EOCs-functionalised particles allowed us to observe the effect of equivalent concentrations of each compound on HepG2 cells' viability. Eugenol and vanillin presented a lesser cytotoxic effect in their free form than when immobilised on silica particles' surfaces. Chen et al. (2009) studied the cytotoxic effect of chitosan nanoparticles functionalised with eugenol and carvacrol. Unlike the results reported herein, cytotoxicity assays using 3T3 mouse fibroblast showed that both the eugenol and carvacrol functionalised particles were significantly less cytotoxic than free EOCs. Other than the characteristics of the starting material could be responsible for these differences. As previously mentioned, major differences have been found in the IC_{50} values of eugenol in different works depending on the employed cell type. These authors reported that eugenol caused cell death only at a concentration above 0.31 $\mu\text{g/mL}$ (1.89 μM), while the cytotoxic effects in our study fell

within the milimolar range. Moreover, the degree of grafting achieved for eugenol on chitosan nanoparticles was higher (26.7%) than on MCM-41 nano (6.4%), which was the most efficient eugenol functionalisation reaction in our study. So the substantially lower concentrations of functionalised particles analysed by these authors might also be responsible for the differences that lie in both studies.

The immobilisation of eugenol and vanillin on silica particles has been demonstrated to increase their antimicrobial activity against different microorganisms compared to free components (García-Ríos et al., 2018; Ribes et al., 2019; Ruiz-Rico et al., 2017). Indeed using immobilised compounds lowers the concentration of EOCs required to inhibit microorganism growth and, therefore, the expected differences in the cytotoxic effect between the free EOCs and EOCs-functionalised silica at effective antimicrobial concentrations should also reduce.

The improved antimicrobial effectiveness of immobilised molecules has been attributed to an increased interaction of EOCs with cell membranes, either for the high density of molecules on silica particles' surfaces or the reduced volatility of immobilised compounds (Ribes et al., 2017). These phenomena might also be responsible for the increased cytotoxic response to immobilised compounds because, as with bacteria, the cytotoxicity of EOCs in eukaryotic cells appears to include damage to cell membranes (Bakkali et al., 2008).

By comparing the bare and EOCs-functionalised materials, the obtained results differed depending on particle type. SAS functionalisation did not increase cytotoxicity in HepG2 cells, but cells were more sensitive to the functionalised than the bare MCM-41 particles. Moreover, the SAS functionalised particles had the mildest cytotoxic effect, while the eugenol and vanillin-functionalised MCM-41 micro were the most cytotoxic materials. Similarly to this work, Chen et al. (2009) found increased

cytotoxicity in association with the eugenol and carvacrol functionalised chitosan compared to bare chitosan. The IC₅₀ value found for functionalised chitosan was around 1 mg/mL after 72 h of exposure, while cell viability was over 80% for the higher tested concentration (2 mg/mL) of bare chitosan nanoparticles. Other researchers have also observed increased cytotoxic behaviour of silica materials after different surface chemical treatments (Santos et al., 2010) or by anchoring functional groups, such as amine molecules (Bhattacharjee et al., 2010; Puerari et al., 2019; Ruizendaal et al., 2009; Vicentini et al., 2017) or carboxylic acid groups (Petushkov et al., 2009).

The physico-chemical characteristics of particles are main factors that determine their interaction with biological systems and are, therefore, crucial when assessing toxicity (Bouwmeester et al., 2011). In this study, shape, particle size, zeta potential and degree of functionalisation were analysed to correlate the specific physico-chemical properties of materials with their cytotoxic profiles. As expected, no differences were found in the shape and individual mean diameter size of materials before and after the functionalisation process. However, changes in the surface properties and particle size distribution of materials were observed by introducing new functional groups. In particular, the functionalisation of silica particles with both EOCs led to a shift in the zeta potential values from negative to positive. The change in the charge observed after functionalisation could be interesting because, as cell membranes are negatively charged, a more marked interaction is expected for cationic compared to negatively charged particles (Cho et al., 2012). Indeed different studies have demonstrated that positively charged particles are more cytotoxic than negative or neutral variants of similar sizes in non-phagocytic cells (Bhattacharjee et al., 2010; Ruizendaal et al., 2009). It has been described that while anionic particles may cause intracellular damage, positively charged materials are more prone to produce membrane damage either

directly or by detachment of adsorbed polymers (Fröhlich, 2012). Kurtz-Chalot et al. (2014) compared cellular uptake and toxicity against RAW 264.7 murine macrophages of different degrees of positive, neutral and negatively charged silica nanoparticles coated with amino groups, polyethylene glycol and carboxylic acid groups, respectively. These authors found that the highly positively charged nanoparticles were the most adsorbed on cell surfaces and were the most cytotoxic of different nanoparticle types, while no cellular uptake took place. Moreover, these particles caused the most severe membrane integrity loss and the highest pro-inflammatory signal. These results suggest that adsorption on the cell membrane plays a more important role than nanoparticle uptake in the cytotoxicity of cationic particles. In our study, as all the functionalised materials presented a positive surface charge, but SAS functionalisation did not increase their cytotoxicity behaviour, not only the cationic nature of particles, but also other factors of particles' surface chemistry, may also have an effect. Together with surface charge, the hydrophobicity levels and nature of surface modifications are considered essential for determining different biological effects (Sun et al., 2019). As described for cationic particles, hydrophobic surfaces promote cell-particle interactions and react more cytotoxically than hydrophilic surfaces (Fröhlich, 2012). The hydrophilicity of silica materials is related to the number of silanol groups available to form hydrogen bonds with water molecules (Napierska et al., 2010). The hydrophobicity of EOCs-functionalised materials is no doubt expected to be due to both a decrease in silanol groups on their surface and the hydrophobicity provided by the presence of the alkoxysilane derivatives of eugenol and vanillin anchored to particles. The differences in cytotoxic behaviour observed between the functionalised SAS and MCM-41 materials could, therefore, be explained by the functionalisation yield. This parameter was lower for SAS than mesoporous particles, but no significant differences appeared in

the performance of the functionalisation reaction for both MCM-41 material types. Both the porosity and ordered structure of mesoporous materials provide a suitable platform for the covalent anchoring of organic groups (Moritz & Geszke-Moritz, 2015). Indeed the larger amount of EOCs found in the immobilisation reaction on MCM-41 particles could be attributed to the higher density of silanol groups on their inner and outer surfaces compared to SAS.

The analysis of the particle size distribution of the silica materials showed smaller hydrodynamic size values for the functionalised particles. Certain conditions, such as pH, temperature or ion strength, applied to prepare functionalised materials can change the surface properties of the particles and modify their agglomeration state (Halamoda-Kenzaoui et al., 2017; Schneider & Jensen, 2009), which are responsible for the differences between the bare and functionalised particles. Internalisation of individual silica microparticles has been found in the cytoplasm of different cell lines (Yu et al., 2009), but the cellular uptake of silica has been found in an inverse proportion to their size for non-phagocytic cells, and to depend on the degree of particle aggregation and agglomeration (Rancan et al., 2012; Sakai-Kato et al., 2014). Indeed the highest cellular uptake rate in non-phagocytic cells has been found for nanoparticles between 20 and 50 nm (Fröhlich, 2012). The big hydrodynamic particle size found for the different bare and functionalised materials suggests that the adsorption of particles by HepG2 cells would be negligible, even for MCM-41 nano, given their high agglomeration state in solution.

All this information suggests that the cytotoxicity of modified materials for HepG2 cell is probably due to the physical interaction of particles with cell membranes. The good adhesion of cationic particles has been related to occur by either direct electrostatic interactions with cell membranes (Su et al., 2012) or indirectly through the

protein corona formed on the surfaces of charged particles (Kurtz-Chalot et al., 2014). After adhesion, particles may have different biological effects on cell surfaces, including physical damage of the membrane by focal dissolution or hole formation, interaction with membrane-bound proteins (Fröhlich, 2012) and extracellular ROS generation (Santos et al., 2010). Therefore, these biological effects may be related to the strong cytotoxic effect found for the EOCs-functionalised MCM-41 compared to pristine materials.

In order to quantify and compare the cytotoxic effect of the different functionalised silica particles, the MTT and AB methods were assayed. Concentration- and time-dependent effects on HepG2 viability were observed after exposure to all the tested functionalised materials using both metabolic endpoints. Both methods provided useful information for identifying the *in vitro* cytotoxicity of these materials and it is noteworthy that no interference took place between particles and the AB assay, although subtracting the absorbance of the functionalised particles was necessary in the MTT test. However, MTT was a more sensitive endpoint than AB. This effect was more pronounced for the functionalised SAS, eugenol-functionalised MCM-41 nano and for 24 h exposure to the eugenol-functionalised MCM-41 micro and vanillin-functionalised MCM-41 nano, when no accurate estimation of the IC_{50} values was possible by the AB method. As observed in the comparative study, and independently of the EOCs, the functionalised SAS exerted the least cytotoxic effect against HepG2 cells, while the functionalised MCM-41 micro was the most cytotoxic material. Indeed when comparing the bare and functionalised IC_{50} values, the modified MCM-41 micro had a cytotoxic effect that was around 40-fold stronger than for pristine materials.

By comparing the IC_{50} values of the different silica particles obtained by the MTT assay, no significant differences were found between the cytotoxic behaviour of the

eugenol and vanillin-functionalised materials. As previously explained, the cytotoxic effect of free eugenol was 2-fold higher than the effect found for free vanillin. However in the modified silica particles, these differences may be offset by the functionalisation yield for both EOCs. Vanillin anchoring achieved better results than eugenol anchoring, with differences of up to 5-fold bigger for SAS or 3-fold for MCM-41 micro. Different degrees of steric hindrance have been responsible for differences in the functionalisation yield between EOCs (Chen et al., 2009). In this study, these differences could be due to the lesser efficiency of the formylation process to obtain the aldehyde derivative eugenol as the presence of an aldehyde group in the vanillin structure avoids this first synthesis stage. These results suggest that the number of molecules from the EOCs anchored to silica surfaces is an important factor for determining their cytotoxic behaviour.

This study provides information that clarifies the possible risk which derives from using these new materials in food applications. The obtained results indicate that the eugenol and vanillin-functionalised silica particles exhibited a stronger cytotoxic effect on HepG2 cells than the free EOCs and pristine silica materials. The milder cytotoxic effect found for the functionalised SAS than the functionalised MCM-41 materials seemed to be related to the functionalisation yield. The relation between the physico-chemical properties and cytotoxicity found for the different particle types herein analysed suggest that the mechanism responsible for enhanced cytotoxicity could depend on increased cell-particle interactions to some extent. In fact the properties of the functionalised particles' surface, such as cationic nature and hydrophobicity, seemed the most important factors to determine their interactions with cells and, hence, their cytotoxic behaviour. Basal cytotoxicity data may help to predict the acute toxicological effects of materials for food applications, but further studies are necessary to elucidate

the mechanism of toxicity induced by exposure to these new particles. All this information will help to develop new effective and safer materials for food applications.

Acknowledgements

The authors gratefully acknowledge the financial support from the Spanish government (Project RTI2018-101599-B-C21 (MCUI/AEI/FEDER, EU)). C.F. thanks the *Generalitat Valenciana* for being funded by the predoctoral programme Vali+d (ACIF/2016/139). M.R.R. also acknowledges the *Generalitat Valenciana* for her postdoctoral fellowship (APOSTD/2019/118).

References

- Al-Naqeb, G., Ismail, M., Bagalkotkar, G., & Adamu, H. A. (2010). Vanillin rich fraction regulates LDLR and HMGCR gene expression in HepG2 cells. *Food Research International*, 43(10), 2437–2443.
<https://doi.org/10.1016/j.foodres.2010.09.015>
- Bagheri, E., Ansari, L., Abnous, K., Taghdisi, S. M., Charbgoon, F., Ramezani, M., & Alibolandi, M. (2018). Silica based hybrid materials for drug delivery and bioimaging. In *Journal of Controlled Release* (Vol. 277, pp. 57–76). Elsevier B.V.
<https://doi.org/10.1016/j.jconrel.2018.03.014>
- Bakkali, F., Averbeck, S., Averbeck, D., & Idaomar, M. (2008). Biological effects of essential oils – A review. *Food and Chemical Toxicology*, 46(2), 446–475.
<https://doi.org/10.1016/j.fct.2007.09.106>
- Bantz, C., Koshkina, O., Lang, T., Galla, H.-J., Kirkpatrick, J., Stauber, R. H., & Maskos, M. (2014). The surface properties of nanoparticles determine the agglomeration state and the size of the particles under physiological conditions.

Beilstein J. Nanotechnol, 5, 1774–1786. <https://doi.org/10.3762/bjnano.5.188>

Bhattacharjee, S., de Haan, L. H. J., Evers, N. M., Jiang, X., Marcelis, A. T. M., Zuilhof, H., Rietjens, I. M. C. M., & Alink, G. M. (2010). Role of surface charge and oxidative stress in cytotoxicity of organic monolayer-coated silicon nanoparticles towards macrophage NR8383 cells. *Particle and Fibre Toxicology*, 7(1), 25. <https://doi.org/10.1186/1743-8977-7-25>

Bouwmeester, H., Byrne, H., Casey, A., Chambers, G., Lynch, I., Marvin, H. J. P., Dawson, K. A., Berges, M., Braguer, D., Byrne, H. J., Clift, M. J. D., Elia, G., Fernandes, T. F., Fjellsbo, L. B., Hatto, P., Juillerat, L., Klein, C., Kreyling, W. G., Nickel, C., ... Stone, V. (2011). Minimal Analytical Characterisation of Engineered Nanomaterials Needed for Hazard Assessment in Biological Matrices
Recommended Citation Minimal analytical characterization of engineered nanomaterials needed for hazard assessment in biological matrices. *Nanotoxicology*, 5, 1–11. <https://doi.org/10.3109/17435391003775266>

Braun, K., Stürzel, C. M., Biskupek, J., Kaiser, U., Kirchhoff, F., & Lindén, M. (2018). Comparison of different cytotoxicity assays for in vitro evaluation of mesoporous silica nanoparticles. *Toxicology in Vitro*, 52, 214–221. <https://doi.org/10.1016/j.tiv.2018.06.019>

Calabrese, E. J. (2008). Hormesis: Why it is important to toxicology and toxicologists. In *Environmental Toxicology and Chemistry* (Vol. 27, Issue 7, pp. 1451–1474). John Wiley & Sons, Ltd. <https://doi.org/10.1897/07-541.1>

Chen, F., Shi, Z., Neoh, K. G., & Kang, E. T. (2009). Antioxidant and antibacterial activities of eugenol and carvacrol-grafted chitosan nanoparticles. *Biotechnology and Bioengineering*, 104(1), 30–39. <https://doi.org/10.1002/bit.22363>

Cho, W.-S., Duffin, R., Thielbeer, F., Bradley, M., Megson, I. L., MacNee, W., Poland,

C. A., Tran, C. L., & Donaldson, K. (2012). Zeta Potential and Solubility to Toxic Ions as Mechanisms of Lung Inflammation Caused by Metal/Metal Oxide Nanoparticles. *Toxicological Sciences*, 126(2), 469–477.

<https://doi.org/10.1093/toxsci/kfs006>

Davoren, M., Herzog, E., Casey, A., Cottineau, B., Chambers, G., Byrne, H. J., & Lyng, F. M. (2007). In vitro toxicity evaluation of single walled carbon nanotubes on human A549 lung cells. *Toxicology in Vitro*, 21(3), 438–448.

<https://doi.org/10.1016/j.tiv.2006.10.007>

Diab, R., Canilho, N., Pavel, I. A., Haffner, F. B., Girardon, M., & Pasc, A. (2017). Silica-based systems for oral delivery of drugs, macromolecules and cells. *Advances in Colloid and Interface Science*, 249, 346–362.

<https://doi.org/10.1016/j.cis.2017.04.005>

Efeoglu, E., Maher, M. A., Casey, A., & Byrne, H. J. (2017). Label-free, high content screening using Raman microspectroscopy: The toxicological response of different cell lines to amine-modified polystyrene nanoparticles (PS-NH₂). *Analyst*, 142(18), 3500–3513. <https://doi.org/10.1039/c7an00461c>

EU Commission. (2011a). Commission Regulation (EU) No 1129/2011 of 11 November 2011 amending Annex II to Regulation (EC) No 1333/2008 of the European Parliament and of the Council by establishing a Union list of food additives. *Official Journal of the European Union*, L, 295(4),. <https://eur-lex.europa.eu/legal-content/EN/TXT/PDF/?uri=CELEX:32011R1129&from=ES>

EU Commission. (2011b). Commission Regulation (EU) No 10/2011 of 14 January 2011 on plastic materials and articles intended to come into contact with food. *Official Journal of the European Union*, L,12. <https://eur-lex.europa.eu/legal-content/EN/TXT/PDF/?uri=CELEX:32011R0010&from=EN>

- FDA. (2020). *Electronic Code of Federal Regulations (eCFR)*. Part 182-Substances Generally Recognized as Safe. <https://www.ecfr.gov/cgi-bin/text-idx?SID=e956d645a8b4e6b3e34e4e5d1b690209&mc=true&node=pt21.3.182&rgn=div5>
- Fröhlich, E. (2012). The role of surface charge in cellular uptake and cytotoxicity of medical nanoparticles. In *International Journal of Nanomedicine* (Vol. 7, pp. 5577–5591). Dove Press. <https://doi.org/10.2147/IJN.S36111>
- Fruijtjer- pölloth, C. (2016). The safety of nanostructured synthetic amorphous silica (SAS) as a food additive (E 551). *Archives of Toxicology*, 90, 2885–2916. <https://doi.org/10.1007/s00204-016-1850-4>
- Fuentes, C., Ruiz-Rico, M., Fuentes, A., Ruiz, M. J., & Barat, J. M. (2020). Degradation of silica particles functionalised with essential oil components under simulated physiological conditions. *Journal of Hazardous Materials*, 399, 123120. <https://doi.org/10.1016/j.jhazmat.2020.123120>
- Fujisawa, S., Atsumi, T., Kadoma, Y., & Sakagami, H. (2002). Antioxidant and prooxidant action of eugenol-related compounds and their cytotoxicity. *Toxicology*, 177(1), 39–54. [https://doi.org/10.1016/S0300-483X\(02\)00194-4](https://doi.org/10.1016/S0300-483X(02)00194-4)
- García-Ríos, E., Ruiz-Rico, M., Guillamón, J. M., Pérez-Esteve, É., & Barat, J. M. (2018). Improved antimicrobial activity of immobilised essential oil components against representative spoilage wine microorganisms. *Food Control*, 94, 177–186. <https://doi.org/10.1016/j.foodcont.2018.07.005>
- Giménez, C., de la Torre, C., Gorbe, M., Aznar, E., Sancenón, F., Murguía, J. R., Martínez-Máñez, R., Marcos, M. D., & Amorós, P. (2015). Gated Mesoporous Silica Nanoparticles for the Controlled Delivery of Drugs in Cancer Cells. *Langmuir*, 31(12), 3753–3762. <https://doi.org/10.1021/acs.langmuir.5b00139>

- Halamoda-Kenzaoui, B., Ceridono, M., Urbán, P., Bogni, A., Ponti, J., Gioria, S., & Kinsner-Ovaskainen, A. (2017). The agglomeration state of nanoparticles can influence the mechanism of their cellular internalisation. *Journal of Nanobiotechnology*, *15*, 48. <https://doi.org/10.1186/s12951-017-0281-6>
- Heikkilä, T., Santos, H. A., Kumar, N., Murzin, D. Y., Salonen, J., Laaksonen, T., Peltonen, L., Hirvonen, J., & Lehto, V.-P. (2010). Cytotoxicity study of ordered mesoporous silica MCM-41 and SBA-15 microparticles on Caco-2 cells. *European Journal of Pharmaceutics and Biopharmaceutics*, *74*(3), 483–494. <https://doi.org/10.1016/J.EJPB.2009.12.006>
- Ho, Y.-C., Huang, F.-M., & Chang, Y.-C. (2006). Mechanisms of cytotoxicity of eugenol in human osteoblastic cells in vitro. *International Endodontic Journal*, *39*(5), 389–393. <https://doi.org/10.1111/j.1365-2591.2006.01091.x>
- Holst, C. M., & Oredsson, S. M. (2005). Comparison of three cytotoxicity tests in the evaluation of the cytotoxicity of a spermine analogue on human breast cancer cell lines. *Toxicology in Vitro*, *19*(3), 379–387. <https://doi.org/10.1016/j.tiv.2004.10.005>
- Jaganathan, H., & Godin, B. (2012). Biocompatibility assessment of Si-based nano- and micro-particles. *Advanced Drug Delivery Reviews*, *64*(15), 1800–1819. <https://doi.org/10.1016/J.ADDR.2012.05.008>
- Kurtz-Chalot, A., Klein, J. P., Pourchez, J., Boudard, D., Bin, V., Alcantara, G. B., Martini, M., Cottier, M., & Forest, V. (2014). Adsorption at cell surface and cellular uptake of silica nanoparticles with different surface chemical functionalizations: impact on cytotoxicity. *Journal of Nanoparticle Research*, *16*(11), 1–15. <https://doi.org/10.1007/s11051-014-2738-y>
- Laaksonen, T., Santos, H., Vihola, H., Salonen, J., Riikonen, J., Heikkilä, T., Peltonen,

- L., Kumar, N., Murzin, D. Y., Lehto, V. P., & Hirvonen, J. (2007). Failure of MTT as a toxicity testing agent for mesoporous silicon microparticles. *Chemical Research in Toxicology*, 20(12), 1913–1918. <https://doi.org/10.1021/tx700326b>
- Li, Y., Sun, L., Jin, M., Du, Z., Liu, X., Guo, C., Li, Y., Huang, P., & Sun, Z. (2011). Size-dependent cytotoxicity of amorphous silica nanoparticles in human hepatoma HepG2 cells. *Toxicology in Vitro*, 25(7), 1343–1352. <https://doi.org/10.1016/J.TIV.2011.05.003>
- Moritz, M., & Geszke-Moritz, M. (2015). Mesoporous materials as multifunctional tools in biosciences: Principles and applications. *Materials Science and Engineering: C*, 49, 114–151. <https://doi.org/10.1016/J.MSEC.2014.12.079>
- Mytych, J., Wnuk, M., & Rattan, S. I. S. (2016). Low doses of nanodiamonds and silica nanoparticles have beneficial hormetic effects in normal human skin fibroblasts in culture. *Chemosphere*, 148, 307–315. <https://doi.org/10.1016/j.chemosphere.2016.01.045>
- Napierska, D., Thomassen, L. C., Lison, D., Martens, J. A., & Hoet, P. H. (2010). The nanosilica hazard: Another variable entity. *Particle and Fibre Toxicology*, 7(1), 39. <https://doi.org/10.1186/1743-8977-7-39>
- Peña-Gómez, N., Ruiz-Rico, M., Pérez-Esteve, É., Fernández-Segovia, I., & Barat, J. M. (2020). Microbial stabilization of craft beer by filtration through silica supports functionalized with essential oil components. *LWT*, 117, 108626. <https://doi.org/10.1016/j.lwt.2019.108626>
- Pérez-Esteve, É., Ruiz-Rico, M., de la Torre, C., Villaescusa, L. A., Sancenón, F., Marcos, M. D., Amorós, P., Martínez-Mañez, R., & Barat, J. M. (2016). Encapsulation of folic acid in different silica porous supports: A comparative study. *Food Chemistry*, 196, 66–75.

<https://doi.org/10.1016/J.FOODCHEM.2015.09.017>

Petushkov, A., Intra, J., Graham, J. B., Larsen, S. C., & Salem, A. K. (2009). Effect of crystal size and surface functionalization on the cytotoxicity of silicalite-1 nanoparticles. *Chemical Research in Toxicology*, *22*(7), 1359–1368.

<https://doi.org/10.1021/tx900153k>

Puerari, R. C., Ferrari, E., de Cezar, M. G., Gonçalves, R. A., Simioni, C., Ouriques, L. C., Vicentini, D. S., & Matias, W. G. (2019). Investigation of toxicological effects of amorphous silica nanostructures with amine-functionalized surfaces on Vero cells. *Chemosphere*, *214*, 679–687.

<https://doi.org/10.1016/j.chemosphere.2018.09.165>

Rampersad, S. N. (2012). Multiple Applications of Alamar Blue as an Indicator of Metabolic Function and Cellular Health in Cell Viability Bioassays. *Sensors*, *12*, 12347–12360. <https://doi.org/10.3390/s120912347>

Rancan, F., Gao, Q., Graf, C., Troppens, S., Hadam, S., Hackbarth, S., Kembuan, C., Blume-Peytavi, U., Rühl, E., Lademann, J., & Vogt, A. (2012). Skin penetration and cellular uptake of amorphous silica nanoparticles with variable size, surface functionalization, and colloidal stability. *ACS Nano*, *6*(8), 6829–6842.

<https://doi.org/10.1021/nn301622h>

Reus, T. L., Marcon, B. H., Paschoal, A. C. C., Ribeiro, I. R. S., Cardoso, M. B., Dallagiovanna, B., & Aguiar, A. M. de. (2020). Dose-dependent cell necrosis induced by silica nanoparticles. *Toxicology in Vitro*, *63*, 104723.

<https://doi.org/10.1016/j.tiv.2019.104723>

Ribes, S., Ruiz-Rico, M., Pérez-Esteve, É., Fuentes, A., & Barat, J. M. (2019).

Enhancing the antimicrobial activity of eugenol, carvacrol and vanillin immobilised on silica supports against *Escherichia coli* or *Zygosaccharomyces*

rouxii in fruit juices by their binary combinations. *LWT*, *113*, 108326.

<https://doi.org/10.1016/j.lwt.2019.108326>

Ribes, S., Ruiz-Rico, M., Pérez-Esteve, É., Fuentes, A., Talens, P., Martínez-Máñez, R., & Barat, J. M. (2017). Eugenol and thymol immobilised on mesoporous silica-based material as an innovative antifungal system: Application in strawberry jam. *Food Control*, *81*, 181–188. <https://doi.org/10.1016/J.FOODCONT.2017.06.006>

Ros-Lis, J. V., Bernardos, A., Pérez, É., Barat, J. M., & Martínez-Máñez, R. (2018). Functionalized Silica Nanomaterials as a New Tool for New Industrial Applications. In *Impact of Nanoscience in the Food Industry* (pp. 165–196). Elsevier Inc. <https://doi.org/10.1016/B978-0-12-811441-4.00007-8>

Ruiz-Rico, M., Pérez-Esteve, É., Bernardos, A., Sancenón, F., Martínez-Máñez, R., Marcos, M. D., & Barat, J. M. (2017). Enhanced antimicrobial activity of essential oil components immobilized on silica particles. *Food Chemistry*, *233*, 228–236. <https://doi.org/10.1016/J.FOODCHEM.2017.04.118>

Ruiz, M. J., Festila, L. E., & Fernández, M. (2006). Comparison of basal cytotoxicity of seven carbamates in CHO-K1 cells. *Toxicological and Environmental Chemistry*, *88*(2), 345–354. <https://doi.org/10.1080/02772240600630622>

Ruizendaal, L., Bhattacharjee, S., Pournazari, K., Rosso-Vasic, M., De Haan, L. H. J., Alink, G. M., Marcelis, A. T. M., & Zuilhof, H. (2009). Synthesis and cytotoxicity of silicon nanoparticles with covalently attached organic monolayers. *Nanotoxicology*, *3*(4), 339–347. <https://doi.org/10.3109/17435390903288896>

Sakai-Kato, K., Hidaka, M., Un, K., Kawanishi, T., & Okuda, H. (2014). Physicochemical properties and in vitro intestinal permeability properties and intestinal cell toxicity of silica particles, performed in simulated gastrointestinal fluids. *Biochimica et Biophysica Acta (BBA) - General Subjects*, *1840*(3), 1171–

1180. <https://doi.org/10.1016/J.BBAGEN.2013.12.014>

Santos, H. A., Riikonen, J., Salonen, J., Mäkilä, E., Heikkilä, T., Laaksonen, T., Peltonen, L., Lehto, V.-P., & Hirvonen, J. (2010). In vitro cytotoxicity of porous silicon microparticles: Effect of the particle concentration, surface chemistry and size. *Acta Biomaterialia*, *6*(7), 2721–2731.

<https://doi.org/10.1016/J.ACTBIO.2009.12.043>

Schneider, T., & Jensen, K. A. (2009). Relevance of aerosol dynamics and dustiness for personal exposure to manufactured nanoparticles. *Journal of Nanoparticle Research*, *11*(7), 1637–1650. <https://doi.org/10.1007/s11051-009-9706-y>

Seipenbusch, M., Rothenbacher, S., Kirchhoff, M., Schmid, H. J., Kasper, G., & Weber, A. P. (2010). Interparticle forces in silica nanoparticle agglomerates. *Journal of Nanoparticle Research*, *12*(6), 2037–2044. <https://doi.org/10.1007/s11051-009-9760-5>

Shakeel, F., Haq, N., Raish, M., Siddiqui, N. A., Alanazi, F. K., & Alsarra, I. A. (2016). Antioxidant and cytotoxic effects of vanillin via eucalyptus oil containing self-nanoemulsifying drug delivery system. *Journal of Molecular Liquids*, *218*, 233–239. <https://doi.org/10.1016/j.molliq.2016.02.077>

Sisakhtnezhad, S., Heidari, M., & Bidmeshkipour, A. (2018). Eugenol enhances proliferation and migration of mouse bone marrow-derived mesenchymal stem cells in vitro. *Environmental Toxicology and Pharmacology*, *57*, 166–174. <https://doi.org/10.1016/j.etap.2017.12.012>

Slowing, I., Trewyn, B. G., & Lin, V. S. Y. (2006). Effect of surface functionalization of MCM-41-type mesoporous silica nanoparticles on the endocytosis by human cancer cells. *Journal of the American Chemical Society*, *128*(46), 14792–14793. <https://doi.org/10.1021/ja0645943>

- Su, G., Zhou, H., Mu, Q., Zhang, Y., Li, L., Jiao, P., Jiang, G., & Yan, B. (2012). Effective surface charge density determines the electrostatic attraction between nanoparticles and cells. *Journal of Physical Chemistry C*, 116(8), 4993–4998. <https://doi.org/10.1021/jp211041m>
- Sun, H., Jiang, C., Wu, L., Bai, X., & Zhai, S. (2019). Cytotoxicity-Related Bioeffects Induced by Nanoparticles: The Role of Surface Chemistry. In *Frontiers in Bioengineering and Biotechnology* (Vol. 7, p. 414). Frontiers Media S.A. <https://doi.org/10.3389/fbioe.2019.00414>
- Vicentini, D. S., Puerari, R. C., Oliveira, K. G., Arl, M., Melegari, S. P., & Matias, W. G. (2017). Toxicological impact of morphology and surface functionalization of amorphous SiO₂ nanomaterials. *NanoImpact*, 5, 6–12. <https://doi.org/10.1016/J.IMPACT.2016.11.003>
- Yoshida, T., Yoshioka, Y., Matsuyama, K., Nakazato, Y., Tochigi, S., Hirai, T., Kondoh, S., Nagano, K., Abe, Y., Kamada, H., Tsunoda, S., Nabeshi, H., Yoshikawa, T., & Tsutsumi, Y. (2012). Surface modification of amorphous nanosilica particles suppresses nanosilica-induced cytotoxicity, ROS generation, and DNA damage in various mammalian cells. *Biochemical and Biophysical Research Communications*, 427(4), 748–752. <https://doi.org/10.1016/J.BBRC.2012.09.132>
- Younes, M., Aggett, P., Aguilar, F., Crebelli, R., Dusemund, B., Filipič, M., Frutos, M. J., Galtier, P., Gott, D., Gundert- Remy, U., Kuhnle, G. G., Leblanc, J., Lillegaard, I. T., Moldeus, P., Mortensen, A., Oskarsson, A., Stankovic, I., Waalkens- Berendsen, I., Woutersen, R. A., ... Lambré, C. (2018). Re- evaluation of silicon dioxide (E 551) as a food additive. *EFSA Journal*, 16(1). <https://doi.org/10.2903/j.efsa.2018.5088>

Yu, K. O., Grabinski, C. M., Schrand, A. M., Murdock, R. C., Wang, W., Gu, B., Schlager, J. J., & Hussain, S. M. (2009). Toxicity of amorphous silica nanoparticles in mouse keratinocytes. *Journal of Nanoparticle Research*, *11*(1), 15–24. <https://doi.org/10.1007/s11051-008-9417-9>